論文 / 著書情報
Article / Book Information

Title	Wind-induced Response Characteristic Evaluation of High-rise Seismic Isolated Building Based on Observed Records
Authors	Daiki Sato, Tetsuro Tamura, Yoshiyuki Fugo, Osamu Nakamura, Akira Katumura, Kazuhiko Kasai, Haruyuki Kitamura
Citation	Proceedings of the 14th International Conference on Wind Engineering, , ,
Pub. date	2015, 6

Wind-induced Response Characteristic Evaluation of High-rise Seismic Isolated Building Based on Observed Records

Daiki SATO[1], Teturo TAMURA[2], Yoshiyuki FUGO[3], Osamu NAKAMURA[4],
Akira KATUMURA[5], Kazuhiko KASAI[6] and Haruyuki KITAMURA[7]

[1, 2, 6] Tokyo Institute of Technology, Kanagawa, Japan
[3-5] Wind Engineering Institute, Tokyo, Japan
[7] Tokyo University of Science, Chiba, Japan

email: daiki-s@serc.titech.ac.jp[1], tamura@depe.titech.ac.jp[2], fugo@wei.co.jp[3], nakamura@wei.co.jp[4],
katsumura@wei.co.jp[5], kasai@serc.titech.ac.jp[6], kita-h@rs.noda.tus.ac.jp[7]

ABSTRACT: Number of high-rise seismic isolated buildings increases in Japan. The wind resistant design of the building is done so that the primary members become the elastic-region even if the strong wind forces are acted. In the high-rise seismic isolated building with the low natural frequency, the seismic isolation layer may become plasticity against the strong wind. This paper presents about a long-term dense monitoring system of 20-story high-rise seismic isolated steel building, and discusses about the wind-induced response characteristics of this high-rise seismic isolated building based on observed records.

KEY WORDS: High-rise Seismic Isolated Building; Wind-induced Response; Observation Records; Residual Deformation.

1 INTRODAUCTION

In 1982, the first seismic isolated 2-story house structure having 6 small rubber bearings was built at east of Tokyo, which is called "Yachiyo-dai-house". The number of the isolated building has been gradually increasing after Kobe earthquake in 1995. More than 3000 seismic isolated building were constructed in Japan. Especially, the number of high-rise seismic isolated buildings increases. The wind resistant design of the building is done so that the primary members become the elastic-region even if the strong wind forces are acted. In the high-rise seismic isolated building with the low natural frequency, the seismic isolation layer may become plasticity against the strong wind [1]. The traditional fixed based structures had many experiences of the damage by the not only the huge earthquake but also the strong wind or huge typhoon. However, the investigations of the full-scale researches about the wind-induced response of the high-rise seismic isolated building are not sufficient yet because the isolated structures are new technology and these have been not encountered with the damage by strong wind. Therefore, it is necessary to enhance the observation record to evaluate the wind resistance performance in the high-rise seismic isolation building.

20-story high-rise seismic isolated steel building (91.4 m) as shown as in Figure 1 was constructed at Tokyo Institute of Technology Suzukake-dai campus located in Yokohama Japan in 2005, and a long-term monitoring to the wind velocity and the response of building has been executed. This paper presents about a long-term dense monitoring system of this high-rise seismic isolated building, and discusses about the wind-induced response characteristics of this high-rise seismic isolated building based on observed records.

Figure 1. External appearance of 20-story high-rise seismic isolated steel building (J2-building)

2 HIGH-RISE SEISMIC ISOLATED BUILDING AND CHARACTERISTIC OF OBSERVED WIND DATA

2.1 Outline of high-rise seismic isolated building and monitoring system [1]-[4]

Figure 2 illustrates the elevation of the 20-story seismically isolated building which is called "J2-building", and Figure 3 shows the plan of the isolation floor of J2-building. The foundation and 1st floor of this building are RC structure. The other floors are hybrid with steel beams and CFT columns. In the isolated floor of this building, several types of dampers are installed. 1,200ϕ rubber bearings with conical spring (Figure 4 (a)) are installed in the position A as shown in Figure 3. In the position B, steel dampers (Figure 4 (b)) are set. 1,100 ϕ rubber bearing with the steel dampers (Figure 4 (c), (d)) are installed in the position C and D. In the position E, 1,000 kN oil dampers (Figure 4 (e)) are installed.

So called Mega-Braces (□ - 500 mm x 160 mm x 19 to 32 mm) are installed on the both sides of building because the horizontal stiffness is necessary to maintain the seismic isolation effects. Because this building is very slender shape with the

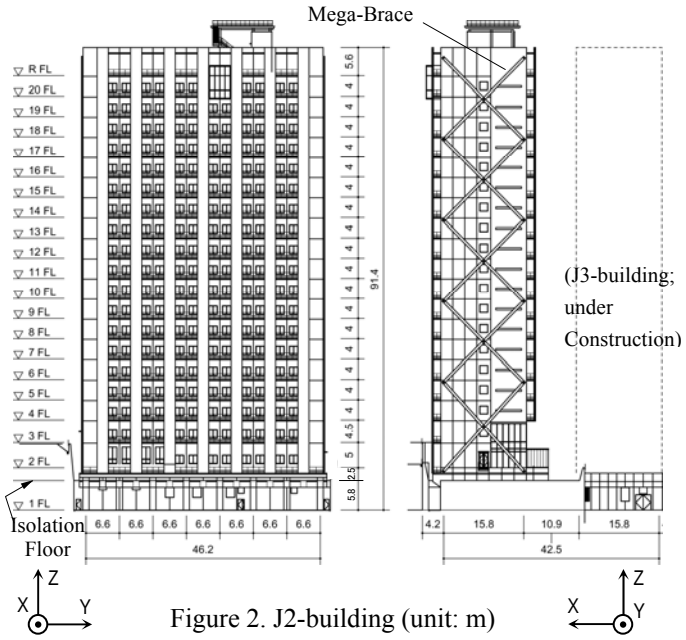

Figure 2. J2-building (unit: m)

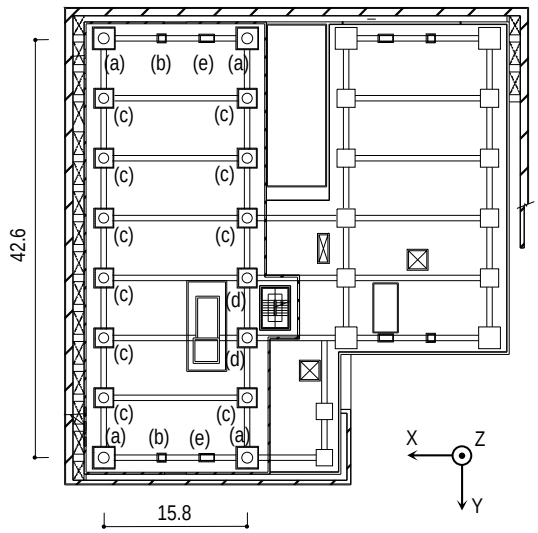

Figure 3. Seismic Isolation Floor (unit: m)

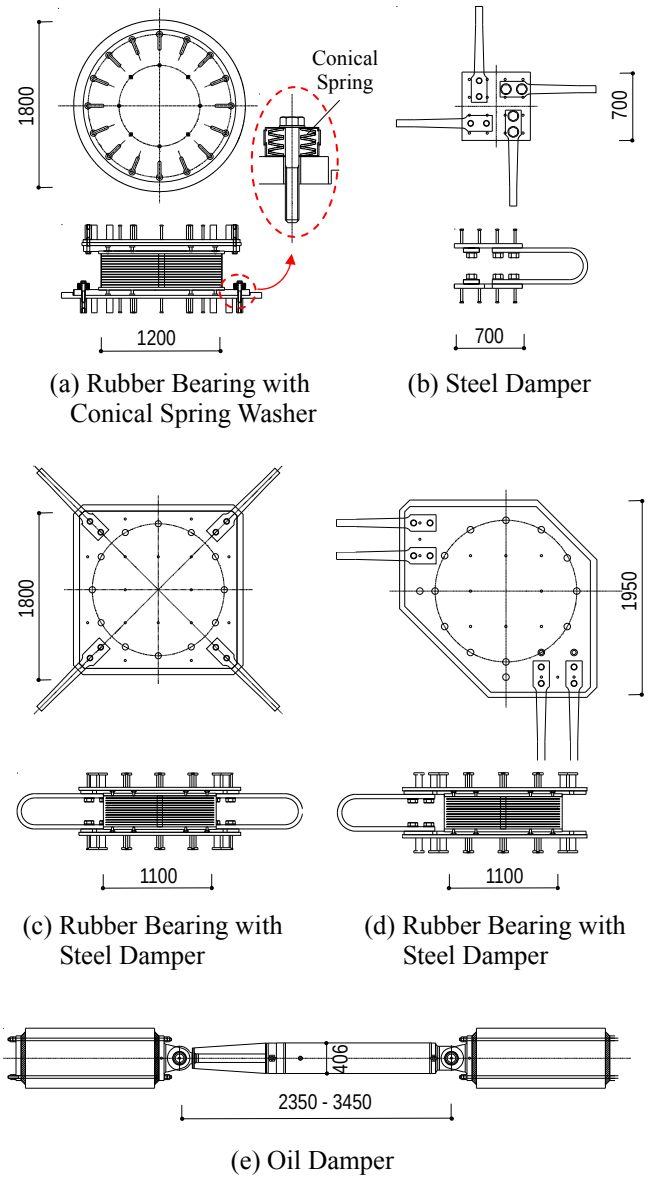

(a) Rubber Bearing with Conical Spring Washer

(b) Steel Damper

(c) Rubber Bearing with Steel Damper

(d) Rubber Bearing with Steel Damper

(e) Oil Damper

Figure 4. Rubber Bearing and Damper (unit: mm)

height of 91.4 m and aspect-ratio of 5, the tensile force in the rubber bearing becomes a critical design problem. If this tall seismic isolated building suffers a major earthquake, the large up-lift forces may develop at the multi-layer rubber bearings due to the tensile force cause by the large overturning moment. To avoid the large tensile forces, the bearings are enabled to do up-lift in this isolated system.

Figure 5 and 6 show the monitoring system, and the list of the sensors are indicated in Table 1. In this long-term monitoring system, the accelerometers are placed on the ground surface, 1st, 2nd, 7th, 14th, 20th floor. This instrument is broad, thus the time history of displacement can be computed by numerical integration. The displacement transducers are installed to measure the displacement of the isolation devices. To measure the large and/or small inter-story displacement in the isolated story level between 1st and 2nd floors, a trace recorder is used in combination with the other measurement devices. The trace recorder is fixed to the steel beam at the bottom of the superstructure while the stainless steel board, on which the behavior of the isolated story is drawn, is fixed to the concrete slab at the top of the substructure. The strain gages are installed at the columns and the Mega-Braces. Oil damper force and deformation are measured. To measure the up-lift of the isolator as shown in Figure 3(a), the displacement transducers and the video camera are placed. Output voltage of accelerometers, displacement transducers and strain gages are A/D converted by data loggers installed at each floor, transmitted to data servers through a LAN, and recorded continuously. The clock on data server is set using a GPS signal data on each data logger via the LAN. Two kinds of anemometer (three-cup anemometer and ultrasonic anemometer) are set up at the top of the building as shown as in Figure 4. The wind speed data averages every three seconds and is recorded as the maximum instantaneous wind speed. The wind

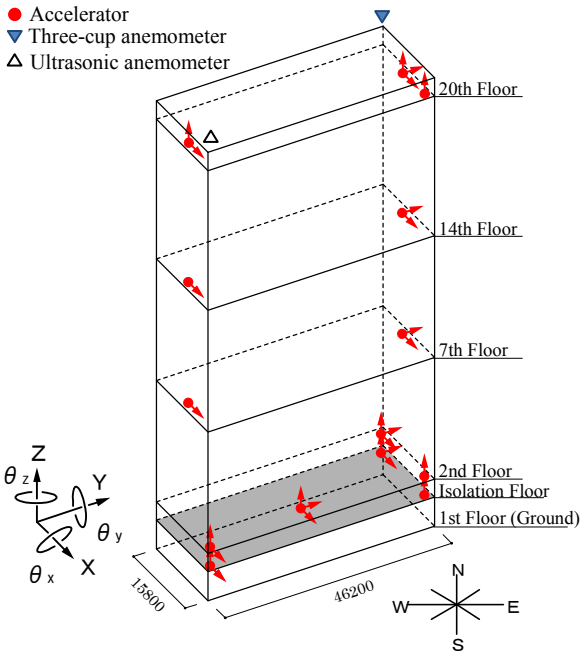

Figure 5. Configuration of accelerators and anemometers

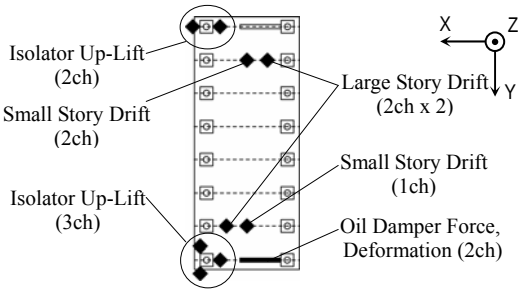

Figure 6. Configuration of displacement transducers at isolation floor

Table 1. List of the sensors

Floor	Item	Capacity	Sensitivity
7, 14, 20F	Acc.	2G	1 μG
	Column, Brace Strain	(Strain Gauge)	1 μstrain
Isolation Floor	Acc.	2G	1μG
	Small Story Drift	±100 mm	0.05 mm
	Large Story Drift	±500 mm	0.5 mm
	Drift Trace	-	-
	Damper Force	(Strain Gauge)	1 μstrain
	Damper Deformation	1000mm	0.5mm
	Isolator Up-Lift	50mm (Video)	0.03mm -
1F	Acc.	2G	1 μG
Ground	Acc.	2G	1 μG

direction is recorded in 16 positive azimuths. The accelerometer, the displacement, the wind speed and direction data are statistically processed every ten minutes in this paper.

2.2 Characteristic of observed wind data

Figure 5 shows appearance frequency of wind direction in the J2-building rooftop from February 2011 to January 2012. Figure 6 shows the turbulence intensity according to the wind direction. The turbulence intensity of 97m on the ground of terrain

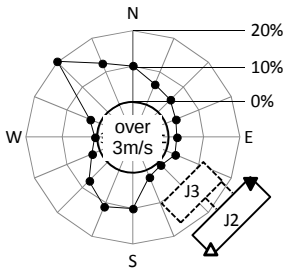

Figure 7. Appearance frequency of wind direction

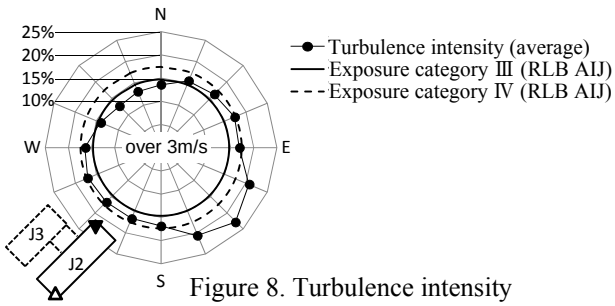

Figure 8. Turbulence intensity

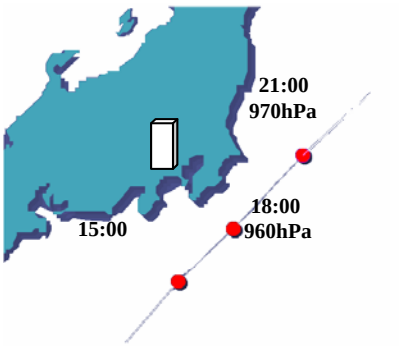

Figure 9. Route of typhoon (T0720; October 27, 2007)

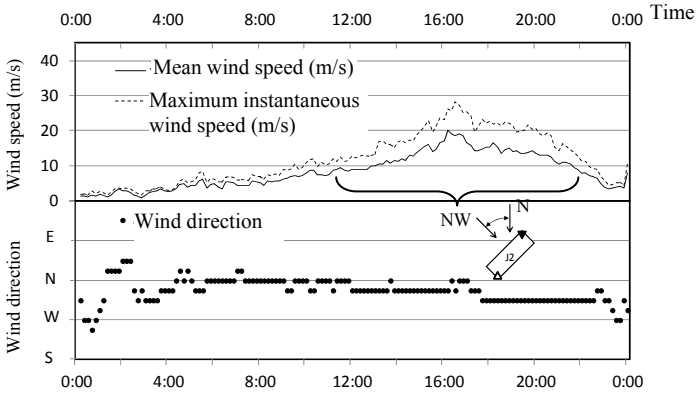

Figure 10. Wind speed and direction

category III and IV in Recommendations for Loads on Buildings Architectural Institute of Japan (RLB AIJ) [5] was described in parallel in this figure. The exposure category indicates the value that corresponds to III or IV in the turbulence intensity in wind directions other than wind direction ESE, SE, and SSE.

Typhoon No.20 in October 27, 2007 (T0720) is described in this paper. Figure 9 shows the route of typhoon T0720. The time history of the mean wind speed, the maximum instantaneous wind speed and the wind direction which are observed by the three-cup anemometer are shown in Figure 10. T0720 typhoon passed over the south of the J2 building, and the wind direction is observed from steady north through a day. The mean wind speed is 20.0 m/s and the maximum instantaneous wind speed is 28.2 m/s, and the return period is about one year [5].

3 RESPONSE CHARACTERISTIC OF BUILDING

3.1 Characteristic of response acceleration

Figure 11 (a), (b) illustrate maximum and standard deviation of observed acceleration of each floor in X and Y direction respectively. These standard deviations are calculated by using 10 minutes data when maximum response is generated at each floor. X direction's response is the twice as large as Y direction, and the top floor response is largest.

The time history of the standard deviation obtained from 10 minutes data in the X, Y and torsional direction [5] acceleration at the top floor of the building are shown in Figure 12. Figure 13 show peak factor of top floor acceleration of each direction. The peak factor is calculated every 10 minutes. The peak factor became about 4-6 in each direction. Figure 14 shows the change in the natural frequency in X, Y and torsional direction. These natural frequencies respectively are obtained from the peak of the power spectrum density of the top floor acceleration on each response directions [5]. It can be verified that each natural frequency has decreased when the strong wind is generated large response occur (see Figure 12). This cause is generated by the deformation of the seismic isolation layer, and described in detail in the next paragraph. Figure 15 shows habitability evaluated

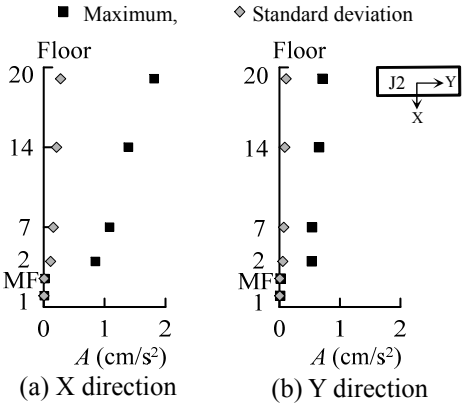

Figure 11. Maximum and standard deviation of observed acceleration of each floor

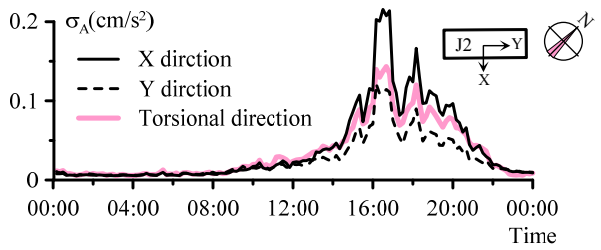

Figure 12. Standard deviation of top floor acceleration σ_A

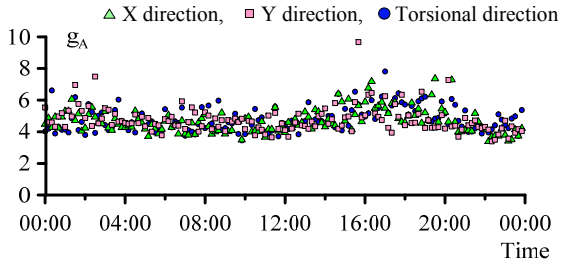

Figure 13. Peak factor of top floor acceleration σ_A

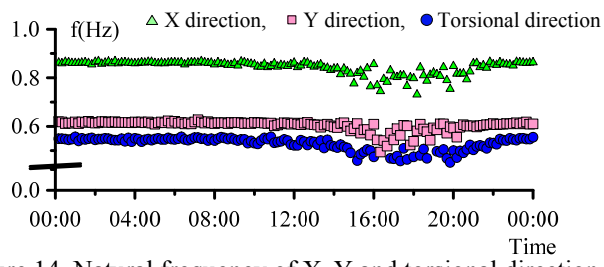

Figure 14. Natural frequency of X, Y and torsional direction

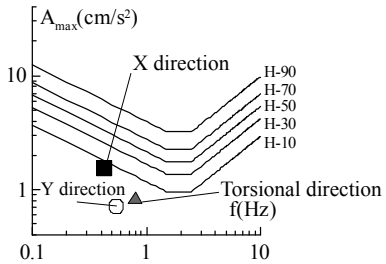

Figure 15. Probabilistic perception thresholds vs. maximum acceleration of top floor A_{max}

based on "*Guidelines for the evaluation of habitability to building vibration* [8]". It can be verified that the probabilistic perception thresholds in the direction of X is smaller than H-10.

Figure 16 (a) - (c) respectively show the relation between the mean wind speed U_H and the standard deviation of the top floor acceleration σ_A at each wind direction; (a) NW, (b) NNW and (c) N. It can be confirmed that a big response occur in X direction compared with the Y direction. In addition, the torsional direction is bigger than Y direction at every wind direction. Especially, it is understood that the torsional direction response is bigger than X direction response in the low wind speed in the N wind direction. It is necessary to note not only the translational vibration but also the twist vibration when we evaluate for the flat high-rise seismic isolated building like the J2 building. Figure 17 (a) – (c) respectively show the relation between the mean wind speed U_H and the sharing ratio of *s*-mode of X direction's floor acceleration ${}_s\beta_A$ [7] at each wind direction; (a) NW, (b) NNW and (c) N.

$$ {}_s\beta_A = \frac{{}_s\sigma_A^2}{\sum_{j=1}^{3} {}_j\sigma_A^2} \tag{1} $$

where, ${}_s\sigma_A$: *s*-mode's acceleration standard deviation.

Within the range of more than 10 m/s, it can be confirmed that the contribution of 1st mode accounts for 80 – 90 %, it becomes the same tendency in all wind directions.

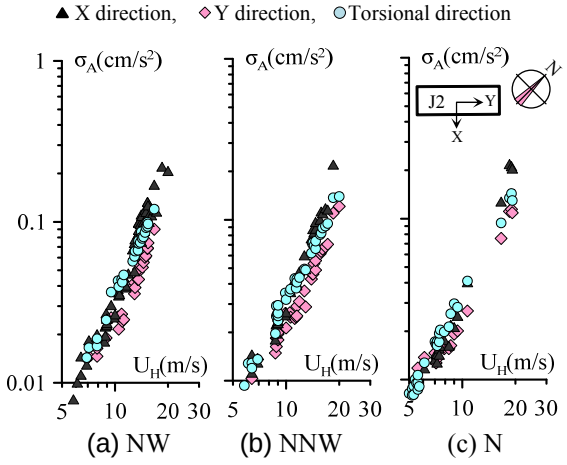

Figure 16. Mean wind speed U_H vs. standard deviation of top floor acceleration σ_A at each wind direction

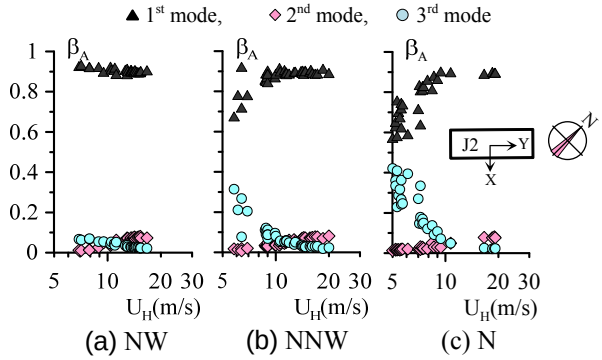

Figure 17. Mean wind speed U_H vs. sharing ratio of each modes of floor acceleration β_A at each wind

3.2 Response characteristics of isolated layer

The deformation of the seismic isolation layer δ_M in X and Y direction are shown in Figure 19. Figure 19 (a) illustrates all record of the typhoon, and Figure 19(b) shows ten minutes around the maximum response in X and Y direction respectively. Maximum deformations are 7.24 mm (X direction) and 2.45mm (Y direction). These deformations are below at yield deformation of the steel damper (31.7mm). Figure 19 shows change of the mean deformation in the seismic isolation layer of every ten minutes in X and Y direction deformation. From Figure 19, it can be verified that the average deformation has changed with the wind direction. Figure 20 shows X-Y deformation-orbit of the seismic isolation layer in ten minutes when the maximum deformation is recorded in X direction. Figure 21 (a), (b) show the relation between the mean wind speed U_H and the

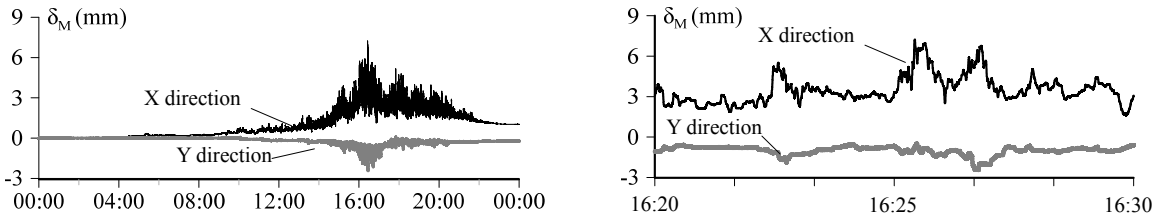

(a) All record (b) Ten minutes (around maximum response)

Figure 18. Deformation of seismic isolation layer δ_M

mean deformation of the isolation layer of X direction δ_{MX}, and Y direction δ_{MY}, respectively. It can be verified that the residual deformation have been generated in X direction.

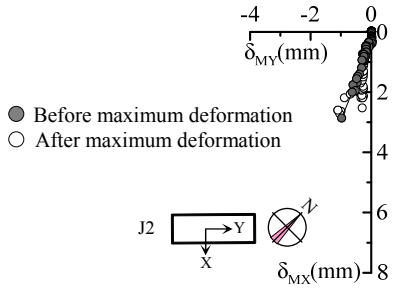

Figure 19. Change in mean deformation of isolation layer (Every ten minutes)

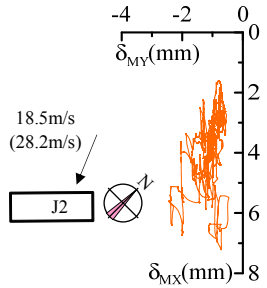

Figure 20. X-Y deformation-orbit of the seismic isolation layer (Ten minutes)

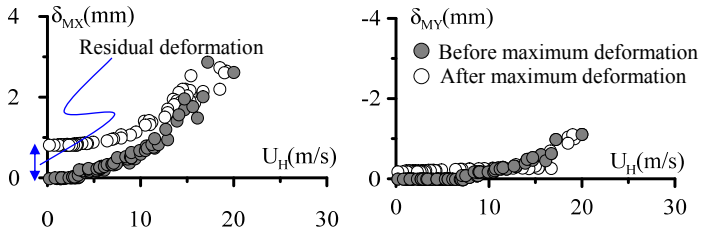

(a) X direction (b) Y direction

Figure 21. Mean wind speed U_H vs. mean deformation of isolation layer δ_M

3.3 Stiffness estimation of seismic isolated layer

The seismic isolation layer's stiffness is estimated by using the observed records in this paragraph. The X direction's static shearing force that acts on seismic isolation layer $Q_{MX}^{(j)}$ is calculated by Eq. (2).

$$Q_{MX}^{(j)} = \frac{1}{2}\rho\left(U_H^{(j)}\right)^2 C_{DX}^{(j)} A^{(j)} \tag{2}$$

where, j : step number every ten minutes, ρ : the air density, $A^{(j)}$: projected area of building at step j, $C_{DX}^{(j)}$: X direction's wind force coefficients at j step's wind direction which are obtained from the wind tunnel experiment. The wind tunnel experiment are carried out by using the exposure category III flow, and the building surroundings are reproduced as shown in Figure 22. Figure 23 illustrates the relation between the X direction deformation of isolation layer obtained from the observer records δ_{MX} and the X direction static shearing force $Q_{MX}^{(j)}$ calculated by Eq. (2). In addition, the designed stiffness of the isolation layer [1]

Figure 22. Situation of wind tunnel experiment

is shown in Figure 23. The stiffness before the maximum deformation of the seismic isolation layer is corresponding to the designed stiffness however the stiffness after the maximum deformation is higher than the design. It can be verified that stiffness is different before and after the maximum deformation. This might be a reason why the residual deformation is generated after the typhoon as shown in Figure 21 (a).

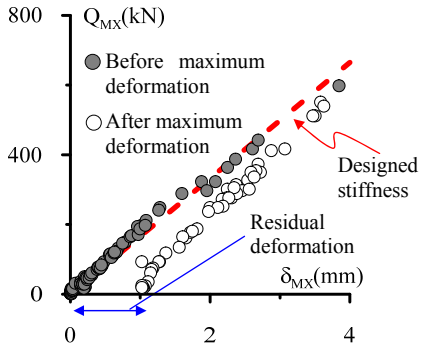

Figure 23. Comparison of X direction's seismic isolation layer stiffness with design and estimation

4 CONCLUSION

The wind-induced response characteristic of the 20-story high-rise seismic isolated steel building constructed at Tokyo Institute of Technology was evaluated based on the observed records in this paper. The obtained findings are described as follows;

1. Torsional response of the building becomes equal with the translational response in some cases, and it is necessary to note not only the translational vibration but also the torsional vibration when we evaluate the wind-induced response such as high-rise seismic isolated building having flat shape.
2. In all wind directions within the range of more than 10 m/s of X direction response, the contribution of the 1st mode response became about 90 %.
3. The residual deformation might be caused after the typhoon because the stiffness of the isolation layer was different before and after the maximum deformation.

ACKNOWLEDGMENTS

This paper is the part of the results of joint-research project by the 21st Century COE program, the Center for Urban Earthquake Engineering (CUEE) in Tokyo Institute of Technology and Kitamura Lab., Tokyo University of Science.

REFERENCES

[1] T.Kikuchi, S.Fujimori, T. Takeuchi and A.Wada, *Design of High Rise Seismic Isolated Steel Building with Mega-Bracing System*, Journal of Technology and Design, Architectural Institute of Japan, No20, 217-222, Dec.,2005 (in Japanese)

[2] Y.Ooki, T.Yamashita, H. Morikawa, S. Yamada, H. Sakata, H.Yamanaka, K. Kasai and A.Wada, *Concrete Approach On Long Term And Dense Monitoring System of Seismically Isolated Tall Building*, Journal of Technology and Design, Architectural Institute of Japan, No21, 73-77, Jun.,2005 (in Japanese)

[3] D. Sato, Y. Ooki, H. Morikawa, S. Yamada, H. Sakata, H. Yamanaka, K. Kasai, A. Wada and H. Kitamura, *Evaluation of Seismically Isolated Tall Building Based on Long-Term Monitoring*, Proceedings of 14th World Conference on Earthquake Engineering, October, 2008

[4] K. Matsuda, K. Kasai, H. Yamagiwa and D. Sato, *Responses of Base-Isolated Building during the 2011 Great East Japan Earthquake*, Proceedings of the 15th World Conference on Earthquake Engineering, September, 2012

[5] *Recommendations for Loads on Buildings*, the Architectural Institute of Japan (AIJ), 2004. http://www.aij.or.jp/jpn/symposium/2006/loads/loads.htm

[6] D. Sato, H. Suzuki, T. Tamura, Y. Fugo, O. Nakamura, K. Kasai and H. Kitamura, *Evaluation of Wind-induced Response of Isolated High-rise Building Based on Monitoring Records*, Proceedings of 22th National Symposium on Wind Engineering , December, 2012. (in Japanese)

[7] H.Hirai, K.Yoshie, D. Sato, Y. Suzuki and H. Kitamura, *Characteristic of Higher Mode Response of High-Rise Building under Fluctuating Wind Force*, Journal of Technology and Design, Architectural Institute of Japan, Vol.18, No38, 79-84, Feb.,2012 (in Japanese)

[8] *Guidelines for the evaluation of habitability to building vibration*, the Architectural Institute of Japan (AIJ), 2004. (in Japanese)